A Hybrid Breast Biopsy System Combining Ultrasound and MRI

C. A. Piron, P. Causer, R. Jong, R. Shumak, and D. B. Plewes*

***Abstract*—System design and initial phantom accuracy results for a novel biopsy system integrating both magnetic resonance (MR) and ultrasound (US) imaging modalities are presented. A phantom experiment was performed to investigate the efficacy of this hybrid guidance biopsy technique in a breast tissue mimicking phantom. A comparison between MR-guided core biopsy verses MR/US-guided core biopsy of phantom targets was realized using a scoring system based on the consistency of the acquired core samples (14 gauge). It was determined that the addition of US to guide needle placement improved the accuracy from an average score of 7.4 out of 10 (MRI guidance alone), to 9.6 (MRI/US guidance) over 21 trials. The average amount of needle tip correction resulting from the additional US information was determined to be 3.7 mm. This correction value is substantial, equal to approximately one radius of the intended targets. Hybrid US/MRI guided biopsy appears to offer a simple means to ensure accurate breast tissue sampling without the need for repeat MRI scans for verification or the need for real-time imaging in open MRI geometries.**

***Index Terms*—Breast biopsy, image registration, interventional radiology, magnetic resonance imaging, stereotactic ultrasound.**

I. Introduction

IT is widely recognized that magnetic resonance (MR)-guided biopsy is a critical element of any breast MR imaging (MRI) capability to ensure optimal patient management [1]–[5]. Currently, there are three main classes of MR breast biopsy systems. The first class relies on a set of prebiopsy MR images to guide delivery of a needle in the fringe field of the magnet based on the use of fiducial markers to reference the position of the lesion. These systems require re-imaging of the breast with the needle in place to verify proper placement [6]–[14]. A second class of real-time biopsy system involves the use of "open-bore" interventional magnets to allow free access to the breast enabling real-time visualization of needle delivery [15]–[18]. A third class of system under development is a "closed-bore" real-time biopsy system [19], [20]. This strategy enables robotic real-time needle guidance for use in high-field MR imaging systems (i.e., $\geq$ 1.5 T) where free access the to patient is not available.

In practice, systems using prebiopsy information do not adequately take into consideration biopsy errors arising from deflection of the needle from its ideal path (i.e., needle wander and/or the movement of the lesion during needle insertion). The real-time interventional "open-bore" MR systems allow for needle positioning error correction, however, the limited number of such systems reduces their use for breast biopsy applications. Furthermore, these open geometry systems are limited to low field strengths thereby reducing image quality. On the other hand, real-time "closed-bore" systems with robotic needle guidance have been designed for use with the more widely available high-field MR systems addressing both these issues. Nevertheless, these systems have only been demonstrated in breast phantom models thus far and there may exist limitations associated with clinical use such as restricted access to regions of the breast (i.e., lesions located near the chest wall) as well as anxiety issues associated with lack of direct contact between the radiologist and the patient.

An alternative biopsy strategy for MR-detected lesions that are occult to other screening modalities is performing a directed, or retrospective US biopsy [21]. This technique uses the position and characteristic features of a lesion in the MR images to locate the lesion in a directed US imaging procedure. This biopsy strategy is preferred as US is commonly used as a real-time needle guidance imaging modality. However, there are problems associated with this technique. The first problem arises from the two dissimilar patient positions used for both imaging procedures. Typically, MR imaging is performed with the patient laying prone with breasts compressed in a medial/lateral configuration, compared with the preferred semi-supine position for US imaging. This leads to difficulties in transferring lesion position from MR to US. Another difficulty arises when a radiologist tries to find a lesion detected with MRI in an US image when normal tissue or other lesions in the vicinity look similar. Furthermore, small lesions, or lesions presenting subtle US features may be easily overlooked when scanning through a large breast volume. When lesions are detected in US, contrast difference from normal tissue may make them difficult to visualize, while matching the orientation of the lesion in US and MR can be problematic. A final problem is related to the time required to

Manuscript received October 15, 2002; revised April 14, 2003. This work was supported in part by the National Cancer Institute of Canada under a Terry Fox Program Project and in part by the Canadian Foundation for Innovation (CFI) through the Ontario Research Development Challenge Fund (ORDCF). This work was presented at the IEEE Ultrasonics Symposium 2001 (Atlanta, GA) as an oral presentation. The Associate Editor responsible for coordinating the review of this paper and recommending its publication was M. W. Vannier. *Asterisk indicates corresponding author.*

C. A. Piron is with the Department of Medical Biophysics, Sunnybrook and Women's College Health Science Centre, University of Toronto, Toronto, ON M4N 3M5, Canada.

P. Causer and R. Jong are with the Department of Medical Imaging, Sunnybrook and Women's College Health Science Centre, University of Toronto, Toronto, ON M4N 3M5, Canada.

R. Shumak was with the Department of Medical Imaging, Sunnybrook and Women's College Health Sciences Centre, Toronto, ON M4N 3M5, Canada. She is now with Cancer Care Ontario, Toronto, ON M5G 2L7, Canada.

*D. B. Plewes is with the Department of Medical Biophysics, Sunnybrook and Women's College Health Science Centre, University of Toronto, Toronto, ON M4N 3M5, Canada (e-mail: don.plewes@sw.ca).

Digital Object Identifier 10.1109/TMI.2003.816951

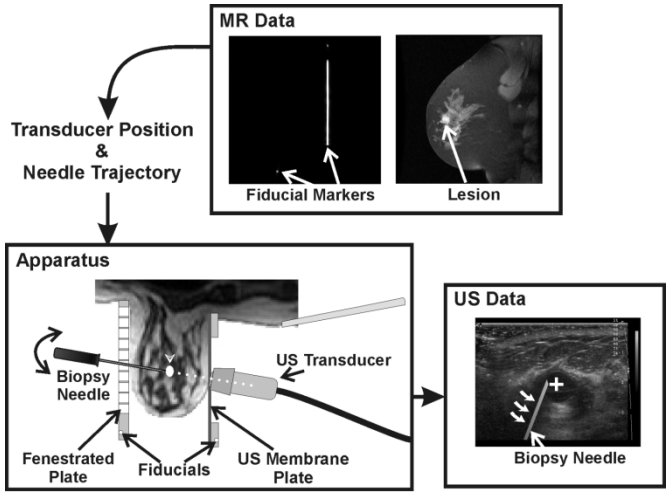

Fig. 1. Hybrid Biopsy Procedure: The breast of interest is shown compressed between medial/lateral plates (bottom left) and imaged using contrast-enhanced MRI (top right). Lesion coordinates and fiducial marker positions in the MR images are entered into a software program that determines needle trajectory and US transducer orientation. These values are calculated such that the lesion is centered in the US images facilitating monitoring of the needle as it advances into the breast (bottom right).

locate the lesion. It is highly dependent on operator skill. Even with these problems, retrospective biopsy using directed US is standard practice. A method that could more accurately and reliably register the US imaging plane with the MR detected lesion would be tremendously beneficial and may provide a solution to the problem of MR-guided biopsy.

In an attempt to address problems associated with current MR-guided and second-look US biopsy strategies, we have developed a hybrid biopsy system based on the standard closed-bore MR magnet configuration, merging prebiopsy MRI information and real-time US information in one procedure. The prebiopsy MRI information is used to determine the needle entry location, trajectory of the biopsy needle and position of a US transducer as demonstrated in Fig. 1. By performing US imaging with the patient in the same conformation as MR image acquisition and using MR information to direct the US probe, one can reduce the uncertainty that the lesion sampled is in fact the same lesion identified in the MR images.

In operation, the patient lies prone on a biopsy frame in which her breasts are immobilized between two compression plates, each supporting a breast coil for MR imaging. A lateral compression plate is fenestrated allowing for positioning of a biopsy plug, which acts to guide a biopsy needle at a defined angle. A medial compression plate has a thin acoustical membrane, which enables US imaging. This system ensures that the location of the lesion as seen in MRI is identical to that of the US image. Thus, even when a lesion is not seen in the US image, lesion location in the US image frame may be determined by correlation with the MR data. During US imaging, the scan plane is oriented to be co-planar with the needle shaft, lesion, and original MR imaging plane. Monitoring needle movement with US, allows real-time correction of any errors associated with biopsy needle wander or lesion movement as the needle is advanced through the breast. The hybrid biopsy system shown in Fig. 1 effectively integrates MRI and US into one system such that each modality performs the function to which it is best suited.

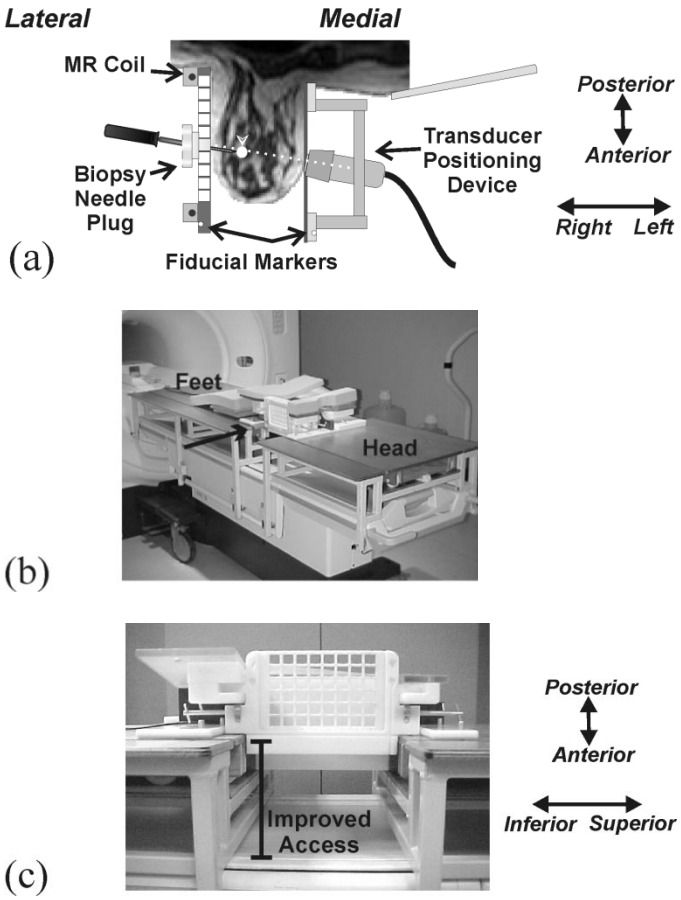

Fig. 2. (a) Schematic of the hybrid biopsy apparatus with transducer positioning device and biopsy guide plug. (b) Image of biopsy apparatus attached to MR magnet. Standard biopsy table has been lowered to enable attachment of system frame. (c) Side view of biopsy apparatus showing improved access provided by frame retrofit.

In this paper, we will review this hybrid biopsy concept, the details of the system design and operation, phantom studies to measure the accuracy of the system and the effect of the hybrid system on biopsy accuracy in breast phantoms. Finally, we review two preliminary MR/US registration cases (one cyst, one carcinoma) to illustrate clinical feasibility.

II. Methods and Materials

A. System Design

The apparatus developed for hybrid biopsy is shown in Fig. 2. This design facilitates access to the breast for both imaging (US and MRI) and intervention. This system was developed by taking advantage of two features of the standard GE MR patient couch (GE Medical Systems, Milwaukee WI), 1) the ability to undock the couch from the imager and 2) the ability to raise and lower the couch. Undocking the couch enables the patient and attached biopsy apparatus to be removed from the magnet room to perform US imaging, while the ability to lower the couch allows the addition of the frame of the biopsy system. This frame performs a similar function as that of the standard GE patient

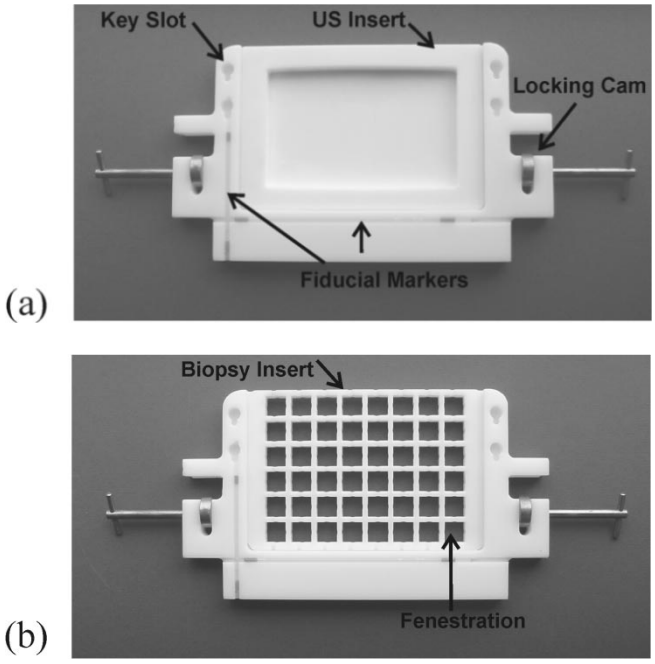

Fig. 3. Compression frames and inserts. Either (a) an US insert or (b) a fenestrated biopsy plate can be accommodated in the compression frames allowing needle access to the breast from with a medial or lateral approach.

couch in guiding the moving tabletop. The frame consists of two sections, which are both rigidly attached to the lowered patient couch; where the volume between the two sections provides access to the breast. On top of the frame, a modified tabletop with the thoracic, cervical patient supports and compression frames attach as shown in Fig. 2(b). The wheels of the tabletop align with alignment rails of the MR magnet. By raising the bed to the correct height and docking the patient bed, the MR imaging system accepts the tabletop as if it were the original. As seen in Fig. 2(c), this design provides improved medial and lateral access to the breast.

Immobilization of the breast is achieved with a pair of frames and interchangeable inserts [Fig. 3(a), (b)]. The frames lock into place along the tracks of the two sections of the biopsy system frame by a pair of locking mechanisms and a set of alignment grooves. These grooves ensure the compression frames are geometrically symmetrical for subsequent stereotactic guidance and localization. The compression frames further contain vertical slots designed to secure both fenestrated biopsy and US compression inserts interchangeably.

The ultrasound (US) insert as shown in a frame [Fig. 3(a)], provides compression of the breast, while allowing US imaging through the acoustical membrane. The insert consists of a frame and a layer of 0.45-mm-thick polystyrene. The composition of the polystyrene is a close match to the acoustical properties of human breast tissue resulting in little attenuation of the acoustic beam in the frequency range of 4–12 MHz as well as little reflection artifact. Alternatively, the breast maybe compressed using the fenestrated biopsy insert [Fig. 3(b)] enabling compression of the breast, while still allowing interventional access through a grid of 1.58-cm-square openings. This design allows access to make a skin incision to facilitate biopsy needle insertion. A biopsy needle may be positioned into the breast through these

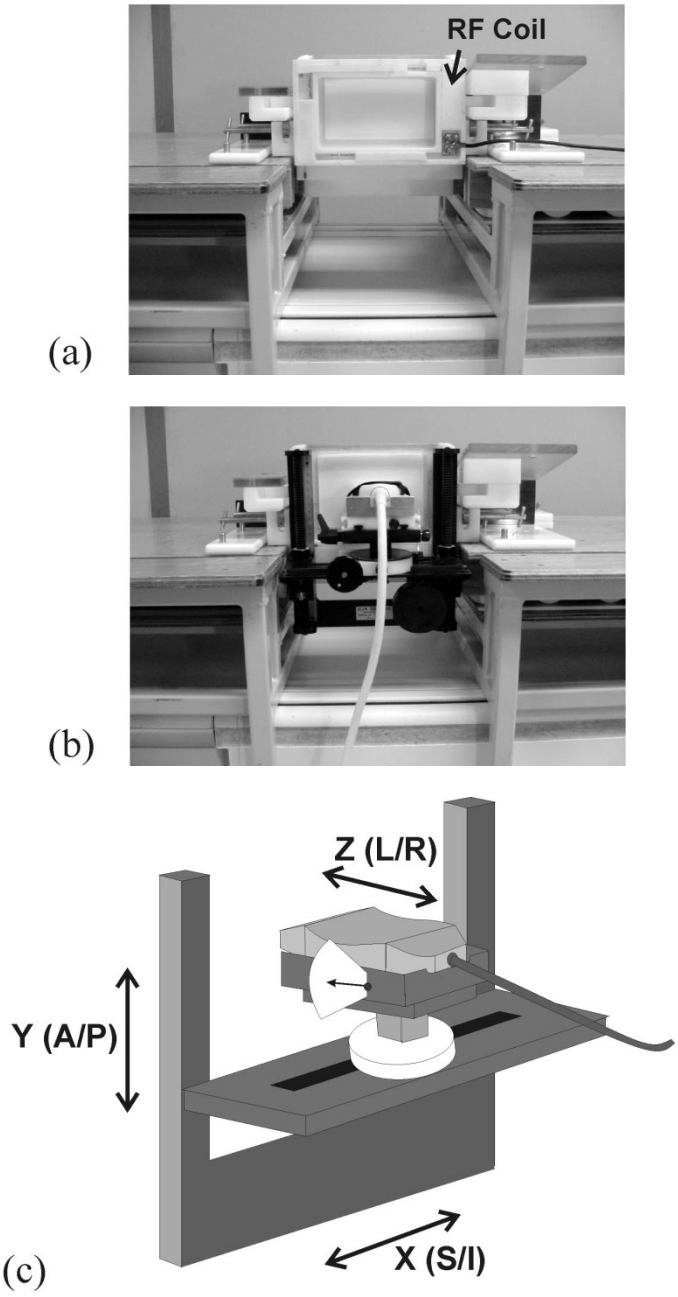

Fig. 4. (a) Lateral view of biopsy apparatus with MR imaging coil attached. (b) Same view with coil detached and US transducer positioning device attached. (c) Oblique schematic of US positioning device. Arrows indicate degrees of freedom of motion.

slots by either freehand guidance, or positioned using a needle guide plug with a stereotactic needle delivery.

A pair of fiducial markers consisting of 3.5-mm-diameter tubes filled with a solution of distilled water and gadolinium are located in a pair of slots milled at known positions in the compression frame. A pair of key slots have also been milled into the frame at specific heights relative to the fiducial marker slots and indicated on Fig. 3(a). These slots accommodate pins of matching geometries enabling attachment of MR imaging coils, or an US transducer positioning system, Fig. 4(a), (b). This positioning system enables 5-degree of freedom positioning of an US transducer, Fig. 4(c). The acoustic beam of a transducer

can be delivered to an MRI detected target in a manner similar to current stereotactic systems using the fiducial markers as a reference point between the MR data and the physical apparatus [14], [22]. By using MRI to locate the fiducials, an appropriate transducer position can be determined such that the target will be located in the middle of the transducer imaging field. This same stereotactic strategy extends to the delivery of a biopsy needle to intercept a target. Accurate definition of an angulated needle trajectory is achieved by way of a specially designed biopsy plug and goniometer. By defining two angles and a needle depth, as shown in Fig. 5, a biopsy needle trajectory can be defined by setting the biopsy plug orientation using the goniometer and locking the needle guide shaft into position. In this manner, a biopsy needle tip can be positioned accurately throughout a biopsy volume and by unlocking the plug, the needle orientation can be modified by free-hand. It is important to point out that stereotactic delivery of the biopsy needle to the target only assists in positioning the needle to approximately the center of the lesion as a first guess based on the MR data. The US registration remains the component that is fundamental to accurate needle delivery to correct for displacements of the target and the needle that could not otherwise occur when using a strictly MR-guided needle positioning strategy. The accuracy of both biopsy needle and US transducer stereotactic positioning techniques are examined in Section II-C.

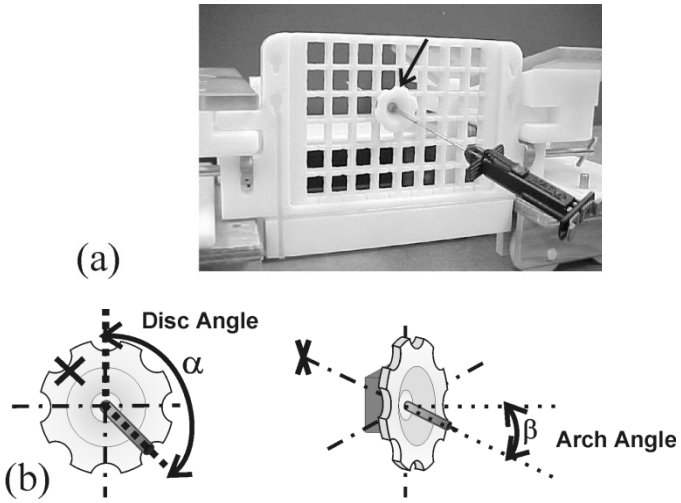

Fig. 5. (a) Fenestrated compression frame with biopsy plug (arrow). (b) The needle guide shaft orientation is defined by two angles as indicated. The shaft can be set and locked into position defined by these two angles using a specially designed goniometer.

B. Clinical Procedure

A candidate for this procedure would be a patient presenting a suspicious lesion on screening MRI that was occult to other imaging modalities. The breast and the approximate position of the lesion in the breast are determined from the previous screening examination. The patient is positioned in the apparatus so that the breast containing the lesion is compressed between two compression frames while a flexible plastic member compresses the contralateral breast against the chest. In this position, the patient is tilted at an angle of approximately 10° from horizontal allowing access to the breast of interest from the medial direction [Fig. 2(a)]. A pair of MR imaging coils are affixed to the apparatus compression frames and the patient is advanced into the MR magnet. The breast is then imaged with two different types of MR pulse sequence sets. The first determines the position of the fiducial origin on the apparatus relative to the breast, while the second is done in conjunction with the injection of gadolinium for lesion visualization. The breast is imaged using the second MR sequence in a dynamic fashion over the entire volume of the breast until the lesion is identified [23]. The lesion and fiducial marker coordinates are identified in the resulting MR images and recorded. Calculations are performed using these values to determine the parameters that define the appropriate transducer position and biopsy needle trajectory such that the shortest needle approach to the lesion is chosen. All calculations are based on vector arithmetic corresponding to the distance between the lesion, the medial plate and lateral plate fiducial origins. Calculations are performed by a software program that first determines the shortest approach (medial or lateral) to the lesion in the left/right (L/R) direction. Using this approach and given that the fiducial markers are at a fixed position relative to the compression plate fenestrations, the fenestration closest to the lesion in the anterior/posterior (A/P) and superior/inferior (S/I) direction is determined. Using this fenestration, the two angles and needle depth required to position the biopsy needle to the center of the lesion are calculated as defined in Fig. 5. The transducer position is determined by defining the angle of the transducer in the A/P, L/R plane to correspond with the projection of the needle trajectory onto that plane. The A/P transducer position is defined so that the imaging plane intercepts the lesion center [Fig. 2(a)], while the S/I transducer position is calculated such that the lesion appears at the center of the US images.

The patient couch is detached from the MR imager and removed from the MR magnetic field into an adjoining room to prepare for the biopsy. The patient remains in the apparatus with her breast firmly compressed and gently transported from the magnet room, taking care not to move her position relative to the apparatus frame. Any movement of the breast would negatively impact the accuracy of the procedure. Once out of the magnet room, the MR surface coils are removed and an US positioning system is attached to the breast compression framework as previously shown in Fig. 4. This system is used to hold the US transducer, which is moved to a predetermined location calculated from the MR fiducial measurements. The US imaging plane is chosen to be co-linear with the calculated biopsy needle trajectory and the lesion and co-registered with the MRI such that the lesion will appear at the center of the US images, at a known depth. The biopsy plug is set to the appropriate trajectory to provide a first guess to intercept the lesion. A small incision is made in the breast at the center of the appropriate fenestration to facilitate needle entry. The biopsy needle is then introduced into the breast via this plug. Any needle trajectory compensations can be made by the operator by unlocking the biopsy plug and correcting the needle trajectory guided entirely by US imaging. Alternatively, the operator could dispense with the biopsy plug and simply introduce the needle through the fenestrations of the biopsy plate. Multiple biopsy samples can be

acquired using either the biopsy plug assisted needle positioning technique, or a free-hand strategy through the same skin incision point, in a manner similar to stereotactic mammography and current US-guided biopsy strategies.

C. System Validation/Characterization

The accuracy of this hybrid biopsy system was characterized using targeting experiments to measure needle positioning and MR/US registration accuracy, as well as breast tissue mimicking phantom experiments to quantify the benefit of real-time US to improving MR-guided biopsy accuracy. All MR imaging was performed on a CVMR 1.5T Signa system (GE Medical Systems, Milwaukee, WI), while all US imaging was performed on an ATL HDI-5000 (ATL Inc, Bothwell, WA) using either a linear array 4–7 MHz transducer (L7-4, ATL) or 5–12 MHz transducer (L12-5, ATL).

Needle Positioning Accuracy: An experiment was performed to determine core biopsy needle positioning accuracy under MRI guidance using the apparatus and technique presented. A targeting apparatus was used to position an MR-visible target within a 160 $\times$ 120 $\times$60 mm volume (S/I, A/P, L/R). This targeting apparatus comprised of a platform rigidly attached to the compression frames, a rod and an MR-visible target. The platform contained an array of holes, spaced at 2.0-cm centers distributed across a plane defined in the L/R, S/I directions. Each of these holes accepts a rod with an MR-visible target attached to the lower portion. This rod was positioned at various depths relative to the platform in the A/P direction. The target used was a plastic pointer used in neurological biopsy procedures (Navigus stem, Image Guided Neurologics Inc. Melbourne, FL). The Navigus stem is a tapered tube (8.5 cm long, 5-mm diameter tapered to 2-mm diameter at tip), filled with a gadolinium and water mixture. The pointed tip of the stem provided a physical target corresponding to a position 5 mm lower than the contained MR-visible fluid.

A single trial involved fixing the target at an arbitrary position, determining the target and fiducial marker positions using three separate T1-weighted spin-echo MR imaging sequences (TR/TE, $\mathrm{N_{PHASE}/N_{FREQUENCY}}$, FOV; 350/14 ms, 128/256, 24 cm), each with the phase encoding direction selected along the measured coordinate to avoid shifts due to magnetic susceptibility variation. These positions were entered into a computer program to determine the appropriate needle trajectory, then positioning a needle to intercept the target tip. The magnitude of the needle positioning error was measured directly with a mechanical caliper with a precision determined to be ± 0.2 mm from repeated experiments. This precision was limited by the ability to define the physical position of the target and the biopsy needle. This needle positioning procedure was preformed 26 times, distributed throughout the biopsy volume on the left (13 trials) and right (13) side of the apparatus, using both lateral (13) and medial (13) approaches.

MR/US Registration Accuracy: A second targeting experiment, using a specially designed water-tank phantom with plastic beads as targets [Fig. 6(a), (b)] was used to characterize the accuracy of MR/US image registration. The targets were spherical plastic beads of various diameters (4, 6, and 8 mm), suspended in a tank of gadolinium-doped degassed water. The speed of sound of the phantom was assumed equivalent to that of breast tissue as a first approximation. The objective of this experiment was to identify bead centers via signal voids in MR images, then use the stereotactic registration technique to position an US transducer [Fig. 6(c)] so the bead appears at a calculated depth in the center of the US image. MR imaging involved three T1-weighted spin-echo sequences (TR/TE, $\mathrm{N_{PHASE}/N_{FREQUENCY}}$, FOV; 350/14 ms, 256/256, 25 cm) used to determine bead and fiducial marker coordinates. Again, in each sequence, the phase encoding direction was selected to avoid shifts due to magnetic susceptibility variation. After MR imaging, the biopsy apparatus was removed from the magnet room for US imaging. A computer program was written which used the MR data to locate the position of each bead in the phantom and to position the US positioning system so that the bead should appear at a known position in the US field. For each bead location, the US transducer was appropriately positioned and the bead coordinate from the US images were recorded. By comparing the expected MR location of the bead to that seen on the US image, we could calculate a registration error. Misregistration error in the X (lateral), Y (elevation), Z (axial) directions corresponding to MR directions S/I, A/P and L/R, respectively, was first determined by re-positioning the transducer in the Y, or elevation direction, until the echo from the front edge of the bead was brightest. The actual Y position of bead was recorded from the scale of the positioning system at this point. The accuracy with which the Y position could be determined was limited by the resolution of the US transducer in the elevation direction and the curvature of the target bead. It was found that the Y position could be defined with a precision of approximately ± 0.5 mm as determined by repeated measurements. The axial, or Z position was measured using the software caliper function on the US system as the distance from the front of the transducer imaging field to the center of the bead. The center of the bead was defined by locating the front edge of the bead and moving the cursor 1 bead radius toward the bead as the back of the bead could not be reliably located. The mid-line shift, or X position was measured from the side of the US image to bead center as indicated in Fig. 6(d). The center of the bead in the X and Z directions could be defined with a precision of approximately ± 0.2 mm as determined by repeated measurements. Error was represented as the absolute value of the difference between the MRI predicted position of the bead and the measured position of the bead in the US images for all directions (X, Y, Z). This registration procedure was performed for a total of 48 targets distributed throughout a 150 $\times$150 $\times$60 mm volume (S/I, A/P, L/R).

Breast Tissue Mimicking Phantom: A comparison of the accuracy of MR-guided verses hybrid guided biopsy was conducted using breast-mimicking phantoms. These phantoms consisted of a block of agar (5.0% by weight) with a number of pimento filled olives distributed throughout the volume. The agar gel simulated the parenchymal tissue, while the olives simulated breast lesions. The olives were approximately 15 mm and pimento cores approximately 7 mm in diameter. The speed of sound in the block of agar has been reported to be similar to that of human tissue ($\sim$ 1500 m/s), therefore, no attempts

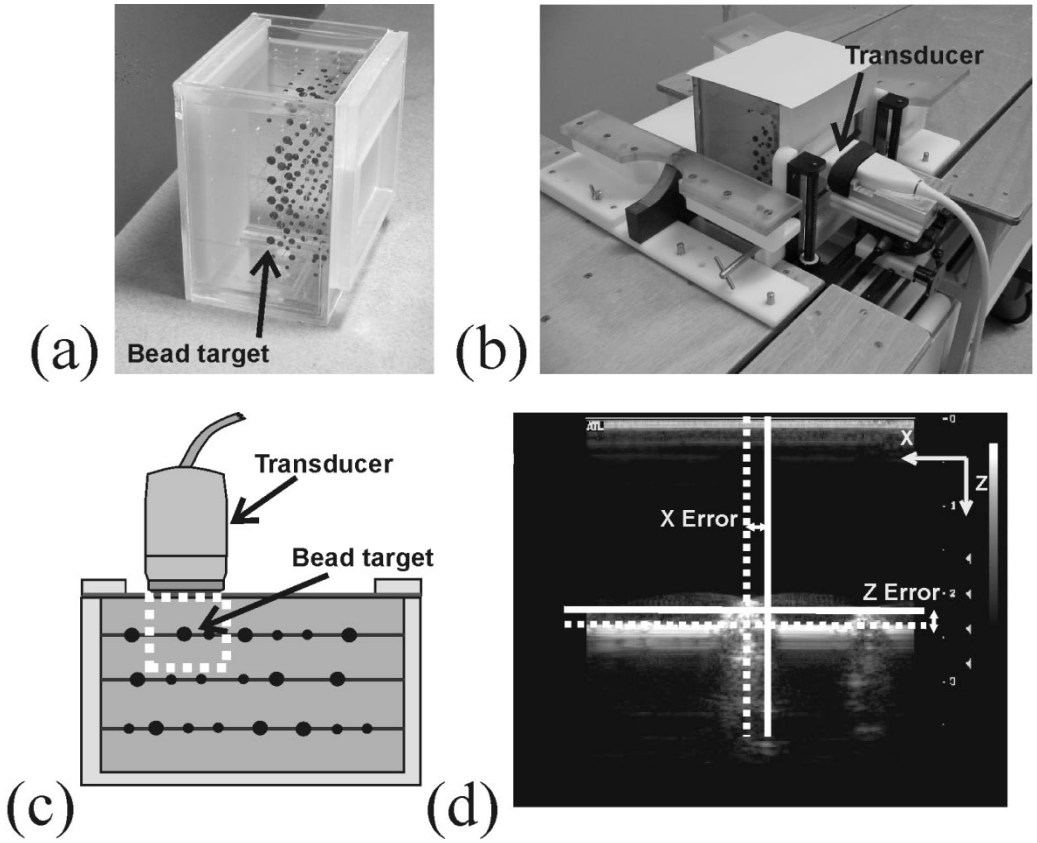

Fig. 6. (a) MRI/US imaging phantom consisting of a series of beads suspended by monofilament in a water tank. The beads appear as voids in the MR images and act as targets for the experiment. (b) US transducer positioned in MR/US registration phantom experiment. (c) Schematic showing the imaging field of the transducer as corresponds to (d). Misregistration X and Z error was measured using the US image using the caliper function on the US system, while the y error was measured by repositioning the transducer in the through-plane direction and recording the new position. The actual bead center is indicated by the intersection of the dashed lines, while the MR calculated center is indicated by the solid lines.

were made to match the speed of sound of the phantom to that of the speed of sound of the US imaging system [24]. MR imaging of the phantom and the fiducial markers was performed using a T1-weighted spin-echo sequence (TR/TE, $\mathrm{N_{PHASE}/N_{FREQUENCY}}$, FOV; 350/14 ms, 128/256, 25 cm), however, identification of the olive target was performed using a sagittal T1-weighted two-dimensional (2-D)-SPGR fat-saturated sequence (TR/TE/flip, $\mathrm{N_{PHASE}/N_{FREQUENCY}}$, FOV; 150 ms/4.2 ms/50°, 128/256, 20 cm).

After MR imaging, the patient table containing the biopsy system and phantom was removed from the magnet room for US imaging using a linear array 4–7 MHz transducer (L7-4, ATL) using the "small parts-breast" system preset. The MR image coordinates of the medial and lateral fiducial origins and the target were entered into a computer script that calculated the biopsy insert fenestration index in the lateral plate, two angles defining the trajectory of the biopsy needle plug guide, the needle depth and the position and angle of the US transducer relative to the medial plate. The angle of a biopsy plug was set using a specially designed goniometer. This plug was positioned in the appropriate biopsy insert fenestration as determined by MRI based calculations. The US transducer was held in place using a positioning apparatus affixed to the medial plate in a manner described in Section II-B. The biopsy needle (14 gauge) was advanced into the phantom while the US images provided real-time visual feedback.

By loosening the biopsy plug and making the appropriate corrections using the US data as a guide, the biopsy needle position could be verified before actuation and subsequent acquisition of the sample as shown in Fig. 7(b). It should be noted that this verification is a 2-D verification of the biopsy needle, which is valid if the needle and lesion remain in the imaging plane of the US transducer. However, in cases where lesion moved, or the needle deflected out of the US plane, repositioning of the US transducer was required. The modified needle position was fixed by tightening the plug and the biopsy gun actuated. The final position of the biopsy needle was used to verify if the biopsy was successful as seen in Fig. 7(c). In order to determine the total amount that the US imaging influenced the biopsy needle positioning, the needle depth before acquiring the sample was recorded and the final trajectory angles of the biopsy plug were measured in the same goniometer used to set the plug trajectories. Using these values, a distance representing the total correction was calculated as demonstrated in Fig. 8(b).

To determine the success of the biopsy, the quality of the core sample was scored (0–10) based on the ratio of pimento, olive and agar in the biopsy sample (see Fig. 9). A biopsy sample of every target in the phantom was obtained using this technique. As a comparison, biopsy samples were obtained from all the targets in the same phantom this time using only the pre-biopsy MRI data. For each biopsy sample obtained, the phantom and fiducial markers were re-imaged using the sequence previ-

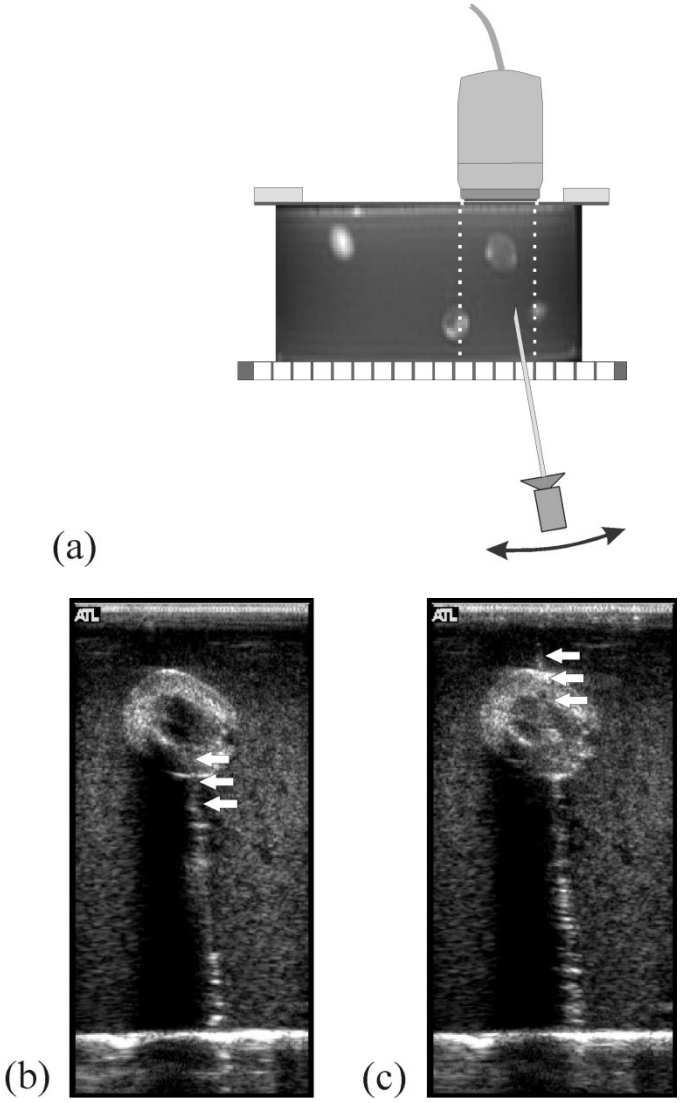

Fig. 7. Needle guidance using US. (a) A coronal view of the phantom and the US transducer. The region enclosed in the dashed white lines correspond to the imaging field of the US transducer in (b) and (c). The prefire position of the needle tip relative to the olive is shown in (b), the postfire position is shown in (c). Slight modifications were made to the needle trajectory based upon the prefire US image.

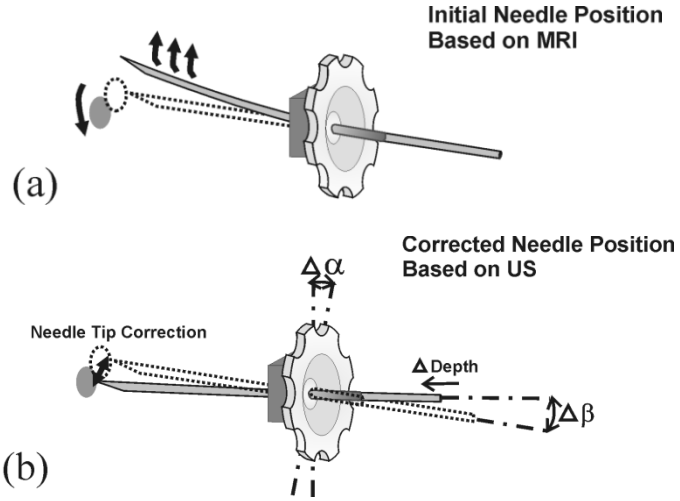

Fig. 8. Measurement of needle tip correction. (a). The top diagram demonstrates the discrepancy between the intended needle position calculated from MR data (dashed outline) and the actual deflected position. Using US images as a guide, the needle tip may be repositioned to intercept the target. The total needle tip correction was calculated by measuring the change in needle depth and change in arch and disc angles by way of the goniometer used to prescribe the plug angles.

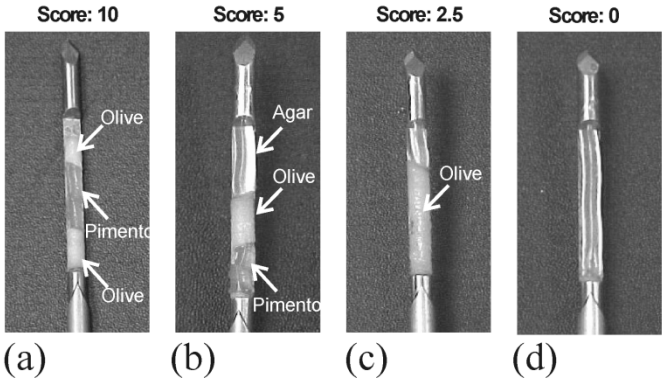

Fig. 9. Biopsy core samples and their respective scores. A perfect score consists of a pimento core surrounded by olive on each side.

ously described. The needle positioning technique and equipment were identical to the hybrid strategy, differing only in the fact that the samples were obtained without the aid of US guidance. No postbiopsy MR images were obtained to verify needle positioning. A total of 21 targets were sampled using both guidance strategies.

MR/US Registration Clinical Application: The MR/US registration portion of the hybrid biopsy procedure was performed in two cases: 1) a patient presenting a cyst on screening US; 2) a patient who presented a suspicious lesion detected during an MRI-screening exam, but was not evident with screening US or mammography. The system previously described was used to target the cyst and lesion in two different patients. The cyst was identified using a sagittal T2-weighted spin-echo, fat-saturated MR sequence (TR/TE, $N_{PHASE}/N_{FREQUENCY}$, FOV, Slice; 3000 ms/98 ms, 128/256, 20 cm, 4 mm) without the use of contrast agent. The lesion was identified using a sagittal T1-weighted 2-D-SPGR fat-saturated MR sequence (TR/TE/flip, $N_{PHASE}/N_{FREQUENCY}$, FOV, Slice; 150 ms/4.2 ms/50°, 128/256, 20 cm, 4 mm) in concert with an intervenous injection of 0.1 mM/kg gadolinium-DTPA. The position of the US transducer was calculated to target the center of these targets, with US imaging performed outside the magnet room. The US transducer used to image the cyst was a linear array 5–12 MHz transducer (L12-5, ATL) with Sono-CT compounding, using the "small parts-breast" system preset, while the transducer used to image the lesion was a linear array 4–7 MHz transducer (L7-4, ATL), again using the "small parts-breast" system preset, without any compounding function.

III. Results

Needle Positioning Accuracy: The resulting average of the magnitude of the error for all trials ($N = 26$) was 1.9 mm, with a standard deviation of 0.7. The maximum needle positioning error was 2.5 mm, while the minimum error was 0.7 mm.

TABLE I
MR/US REGISTRATION TARGETING ACCURACY

	Target registration Error (mm)			Magnitude
	X	Y	Z	Error (mm)
Mean	0.6	0.7	1.0	1.5
Std Dev	0.42	0.56	0.52	0.58
Maximum	2.0	2.5	2.5	3.3

MR/US Registration Phantom Accuracy: Results for the MR/US registration accuracy in the phantom are shown in Table I. The average absolute error across all trials ($\mathrm{N} = 48$) did not exceed 1 mm in any one direction (X, Y, and Z), while the magnitude of the error vector ($\sqrt{X^2 + Y^2 + Z^2}$) was 1.5 mm.

Biopsy Phantom: The average accuracy score for all biopsy procedures ($\mathrm{N} = 21$) using MRI guidance was 7.4 out of a possible 10, compared with an average accuracy score of 9.6 obtained for MRI/US guidance procedures ($\mathrm{N} = 21$). This difference in scores was determined to be statistically significant by the Wilcoxon rank sum statistical test ($\mathrm{P} = 0.022\,75$) [25]. The average needle correction measured for all MRI/US guidance trials was calculated to be 3.7 mm ($\mathrm{P} = 0.0089$). This average amount of needle correction resulting from the additional US information was large relative to the size of these phantom targets (7.0-mm-diameter core) and approximately the size of smaller breast lesions detected using MRI [26].

MR/US Registration Clinical Application: In the first case, a 1-cm cyst was identified using the T2-weighted MR imaging sequence [Fig. 10(a)] and targeted with an US probe using the technique previously described. After positioning the US transducer, a 1-cm cyst was detected, Fig. 10(b). Moving the transducer in the Y, or elevation direction indicated the true center of the cyst was 1 mm from the MRI predicted position. The center of the cyst was 1.5 and 2.0 mm (X, Z directions, respectively) from the MRI predicted position indicated by the crosshairs on Fig. 10(b). Therefore, the magnitude of registration error vector in three-space from the center of the cyst to the MR predicted position was 2.7 mm. In the second case, a rim-enhancing 7-mm lesion was evident during the contrast-enhanced MRI scan (2-D-SPGR, fat-saturated) as seen in Fig. 11(a). The error in the X, Y, and Z directions were 2.0, 1.0, and 2.0 mm, respectively, with the magnitude of the registration error vector calculated to be 3.0 mm. MR-guided wire localization and subsequent pathology determined it to be an invasive carcinoma.

IV. DISCUSSION

We have shown that the positioning errors of our MR-guided needle positioning strategy were less than 2 mm in the absence of any phantom material. The advantages of this system relate to the design of the articulating needle guide. This structure allows for angulated needle entry of the needle and the prospect of gathering multiple needle samples from the same entry point. By virtue of the geometry of the fenestrated square window, it is feasible to apply topical anesthetic to the tissue and make a small tissue incision to facilitate needle entry. The sources of error encountered were primarily due to positional shifts in the MR images due to gradient nonlinearity and uncertainties associated with determining the position of the target and fiducial markers in the MR images due to finite image resolution. On our current MR imaging system, there is a correction algorithm for in-plane gradient nonlinearity errors, however, it is not sufficient for highly accurate determination of position throughout the imaging volume. We anticipate we may correct for these errors in a true three-dimensional sense through offline reconstruction methods [27], [28]. We believe that the contribution of Bo shifts to the error are minor compared with gradient warp, however, misalignment of the apparatus and inaccuracies associated with imprecise machining may contribute more significantly.

Furthermore, we determined in a phantom experiment that MR/US registration error for our system was less than 1.0 mm in all directions. The magnitude of this error vector is small compared with the size of lesion we intend to target in hybrid biopsy procedures ($> 4\ \mathrm{mm}$). We again attribute sources of error to positional errors in the MR images due to gradient nonlinearity, mechanical errors associated with the apparatus and uncertainties associated with the finite resolution of both MR and US images. We believe we can further reduce these sources of error through more careful calibration of the apparatus and application of gradient nonlinearity corrections. Another source of error associated with US imaging further contributed to negatively affect accuracy in this experiment. Our assumption that the speed of sound of the phantom medium (i.e., water) was equivalent to the assumed speed of sound of the US imaging system was too coarse an approximation. The speed of sound of the water is approximately 1490 m/s compared with the US imaging system, which assumes the speed of sound to be 1540 m/s [29], [30]. This inconsistency resulted in shifting the apparent position of the target in the axial direction of the US image approximately 3% further than the actual physical position. Over a distance of 2 cm this lead to an additional error contribution of 0.6 mm in the Z direction. This error was consistent with experimental findings.

We have demonstrated a system which combines real-time US guidance with MR breast imaging to provide a system for accurate MR-guided biopsy. The MR/US registration and needle targeting techniques proved effective in a breast tissue mimicking phantom model. The combination of accurate initial positioning of the biopsy needle, accurate image registration and ability to adjust the position of the needle based on the US images resulted in more accurate core biopsy samples than those obtained with MR guidance alone. The major source of error associated with inaccurate MR-guided biopsy samples was needle deflection due to the stiff agar gel of the phantom whereas the movement of the target within the phantom constituted only a small portion of the error as seen in the US images. The minimal effect of target movement was believed to be due to the medial-lateral compression of the phantom and strong throw of biopsy. It should also be noted that the 2-D nature of US needle guidance is a weakness with this current application as was experienced during the experiments, however, the ability to manipulate the US transducer within its positioning apparatus to adjust for gross lesion and needle deflection proved to be effective.

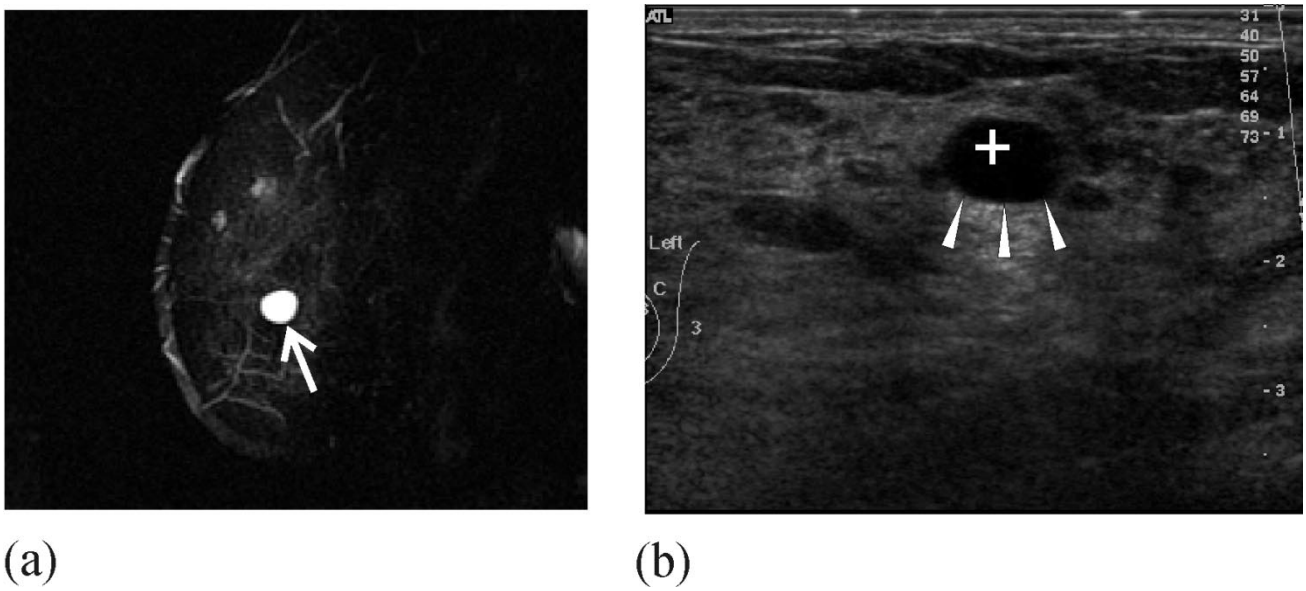

Fig. 10. Clinical application of MR-US co-registration of a cyst (a) 1.0-cm cyst identified with T2-weighted MRI sequence (arrow). (b) Co-registered US image depicting 1.0-cm lesion at a position 2.7 mm from the predicted MRI position (cursor). Registration error was determined to be (X, Y, and Z) 1.5, 1.0, and 2.0 mm.

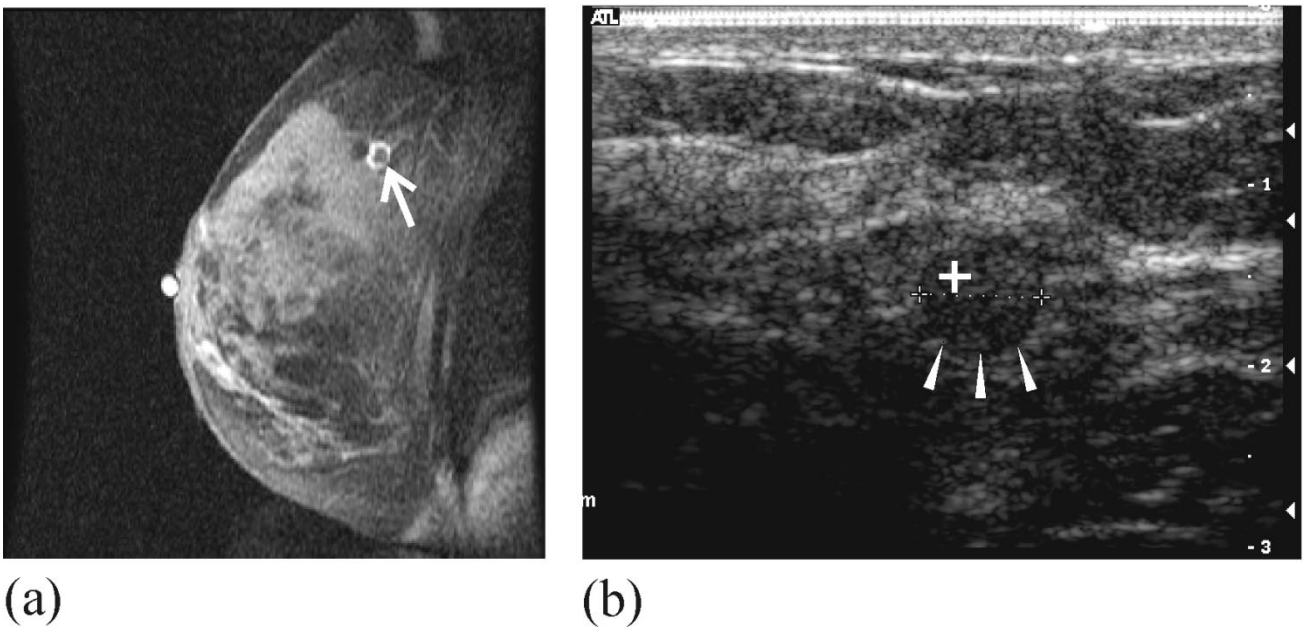

Fig. 11. Clinical Application of MR-US co-registration (a) Rim-enhanced lesion detected with Contrast-enhanced MRI (arrow). (b) Co-registered US image depicting 7-mm lesion at a position 3.0 mm from the predicted MRI position (crosshair). Registration error was determined to be (X, Y, and Z) 2.0, 1.0, and 2.0 mm. This lesion was surgically excised and diagnosed to be an invasive ductal carcinoma.

Our preliminary clinical application of MR/US co-registration demonstrated the feasibility of this technique *in vivo* for both cysts and MR detected lesions. We were able to perform the procedure quickly (under 40 min including equipment setup) and accurately (error less than 3 mm in both cases) in a manner well tolerated by the patient. Our accuracy was negatively affected compared with the phantom experiment as errors associated with patient motion and US imaging in breast tissue became evident. Variations in the speed of sound throughout the breast contribute to warping in the US image [29]. This can be a substantial error as the two extremes of fat and fibroglandular tissue where the speed of sound is approximately 1410 and 1540 m/s, respectively [31]. This results in a substantial misregistration between the physical position of the structures in the breast relative to the transducer and the position of these same structures in the MR image. In the extreme case, with a solid lesion located in a breast composed mainly of fat, there would be approximately an 8% error in the axial position of the lesion. This translates to an error of approximately 1.7 mm at a depth of 2 cm in the breast. This is a substantial error when considered relative to other error sources in the system.

A. Clinical Application

Extending this hybrid procedure to the clinical setting will pose many challenges not experienced in the phantom study. Some potential concerns are patient comfort, breast access, registration accuracy, lesion conspicuity and needle visibility. Thus, far we have found that positioning a variety of patients (i.e., large and small breasted, uni-lateral mastectomy) in the presented manner to be well tolerated by the patient, enabling access to the majority of breast tissue and providing sufficient space for the required apparatus. However, with the current configuration access to tissue regions near the chest wall is somewhat limited. We are currently examining modifications to the current apparatus to improve this aspect.

We also realize that the ability to perform accurate registration of the US plane to the lesion and MR plane in a real breast may be difficult due to patient motion and potential US beam deflection through regions of adipose and fibroglandular tissue. Furthermore, needle visualization in the US images is critically important to ensure proper needle guidance. The strategy presented thus far ensures the needle passes through a minimal amount of breast to reach the lesion. Compromising this requirement by angling the needle trajectory relative to the transducer face may improve needle visibility by generating a stronger reflective signal in the US images. Incorporation of US compounding strategies, which have been shown to improve both lesion and needle conspicuity and are used in common clinical practice, could be easily incorporated into the system as is presented [32].

Finally, lesion visibility in the clinical setting may be the most critical issue. Lesions detected using contrast-enhanced MRI may not be evident in a conventional B-scan US image. The detection of breast cancer using contrast-enhanced MRI is based on tumor angiogenesis, whereas US tumor detection is due to tumor acoustical properties [33]–[36]. A breast tumor may not exhibit properties enabling both MRI and US detection, however, extension of the US imaging mode to Doppler may provide help identify the lesion based on increased blood flow [37], [38]. Optimally the lesion should exhibit some sort of subtle US visible indication, which would allow the radiologist to identify the lesion in the US images when properly registered, however, this is not absolutely necessary.

V. Conclusion

A hybrid-guidance approach to breast biopsy demonstrated to be more accurate than MR guidance alone in a tissue mimicking phantom model. The ability to guide a needle and transducer to a target based on MRI data allows biopsy to be performed in real-time without the need for a specialized MR magnet design. The use of hybrid guidance further offers a reduction in the MRI imaging time and allows utilization of standard, non-MR compatible biopsy tools. Before clinical application of this biopsy strategy, we must address the issues of needle and lesion visibility in the breast. A clinical study is currently underway to evaluate the ability to visualize MR detected lesions using US, nevertheless the preliminary clinical cases presented are encouraging.

Acknowledgment

The authors would like to thank the following individuals for their invaluable assistance in the project: C. Luginbuhl, D. Henderson (DJH Designs), J. Rutledge, E. Ramsay, and R. Walcarius.

References

[1] S. E. Harms and D. P. Flamig, "MR imaging of the breast," *J. Magn. Reson. Imag.*, vol. 3, pp. 277–283, 1993.
[2] J. C. Weinreb and G. Newstead, "MR imaging of the breast," *Radiology*, vol. 196, pp. 593–610, 1995.
[3] L. W. Nunes, M. D. Schnall, and S. G. Orel, "Breast MR imaging: Interpretation model," *Radiology*, vol. 202, pp. 833–841, 1997.
[4] S. H. Heywang-Kobrunner, P. Viehweg, A. Heinig, and C. Kuchler, "Contrast enhanced MRI of the breast: Accuracy, value, controversies, solutions," *Eur. J. Radiol.*, vol. 24, no. 2, pp. 94–108, 1997.
[5] K. C. Kuhl, C. C. Leutner, R. K. Schmutzler, C. C. Leutner, A. Kempe, E. Wardelmann, A. Hocke, M. Maringa, U. Pfeifer, D. Krebs, and H. H. Schild, "Breast MR imaging screening in 192 women proved or suspected to be carriers of a breast cancer susceptibility gene: Preliminary results," *Radiology*, vol. 215, pp. 267–279, 2000.
[6] S. G. Orel, M. D. Schnall, R. W. Newman, C. M. Powell, M. H. Torosian, and E. F. Rosato, "MR imaging-guided localization and biopsy of breast lesions: Initial experience," *Radiology*, vol. 193, pp. 97–102, 1994.
[7] C. K. Kuhl, A. Elevelt, C. C. Leutner, J. Gieseke, E. Pakos, and H. H. Schild, "Interventional breast MR imaging: Clinical use of a stereotactic localization and biopsy device," *Radiology*, vol. 204, pp. 667–675, 1997.
[8] U. Fischer, R. Vosshenrich, D. Keating, H. Bruhn, W. Doler, J. W. Oestmann, and E. Grabbe, "MR-guided biopsy of suspect breast lesions with a simple stereotaxic add-on device for surface coils," *Radiology* , vol. 192, p. 272, 1994.
[9] W. Doler, U. Fischer, I. Metzger, D. Harder, and E. Grabbe, "Stereotaxic add-on device for MR-guided biopsy of breast lesions," *Radiology*, vol. 200, pp. 863–864, 1996.
[10] U. Fischer, R. Vosshenrich, W. Doler, A. Hamadeh, J. W. Oestmann, and E. Grabbe, "MR imaging-guided breast intervention: Experience with two systems," *Radiology*, vol. 195, pp. 533–538, 1995.
[11] B. L. Daniel, R. L. Birdwell, D. M. Ikeda, S. S. Jeffery, J. W. Black, W. F. Block, A. M. Sawyer-Glover, G. H. Glover, and R. J. Herfkens, "Breast lesion localization: A freehand, interactive MR imaging-guided technique," *Radiology*, vol. 207, pp. 455–46, 1998.
[12] S. H. Heywang-Kobrunner, A. Heinig, and R. P. Spielmann, "MR-Guided percutaneous excisional and incisional biopsy," *Eur. Radiol.*, vol. 9, pp. 1656–1665, 1999.
[13] G. P. Liney, D. J. Tozer, and L. W. Turnbull, "Bilateral open breast coil and compatible intervention device," *J. Magn. Reson. Imag.*, vol. 12, pp. 984–990, 2000.
[14] E. Schneider, K. W. Rohling, M. D. Schnall, R. O. Giaquito, E. A. Morris, and D. Ballon, "An apparatus for MR-guided breast lesion localization and core biopsy: Design and preliminary results," *J. Magn. Reson. Imag.*, vol. 14, pp. 243–253, 2001.
[15] H. Sittek, C. Perlet, K. Herrmann, E. Linsmeier, H. Koleum, M. Untch, M. Kessler, and M. Reiser, "MR imaging of the breast. Localization of focal breast lesions with the magnetom open at 0.2 T," *Der Radiologe*, vol. 37, no. 9, pp. 685–691, 1999.
[16] F. A. Jolesz, "Interventional and intraoperative MRI: A general overview of the field," *J. Magn. Reson. Imag.*, vol. 8, pp. 3–6, 1998.
[17] R. B. Lufkin, "Interventional MR imaging," *Radiology*, vol. 197, pp. 16–18, 1995.
[18] S. G. Silverman, B. D. Collick, M. R. Figueria, and F. A. Jolesz, "Interactive MR-guided biopsy in an open configuration MR imaging system," *Radiology*, vol. 197, pp. 175–181, 1995.
[19] W. A. Kaiser, H. Fischer, J. Vagner, and M. Selig, "Robotic system for biopsy and therapy of breast lesions in a high-field whole-body magnetic resonance tomography unit," *Investigat. Radiol.*, vol. 35, no. 8, pp. 513–519, 2000.
[20] N. V. Tsekos, J. Shudy, E. Yacoub, V. P. Tsekos, and I. G. Koutlas, "Development of a robotic device for MRI-guided interventions in the breast," in *Proc. IEEE 2nd Int. Symp. Bioinformatics and Bioengineering Conf.*, 2001, pp. 201–208.
[21] I. M. A. Obdeijn, E. M. J. Brouwers-Kuyper, M. M. A. Tilanus-Linthorst, T. Wiggers, and M. Oudkerk, "MR imaging-guided sonography followed by fine needle aspiration cytology in occult carcinoma of the breast," *AJR*, vol. 174, pp. 1079–1084, 2000.

[22] N. Patoulatos, W. S. Edwards, D. R. Haynor, and K. Yongmin, "Interactive 3-D registration of ultrasound and magnetic resonance images based on a magnetic position sensor," *IEEE Trans. Inform. Technol. Biomed.*, vol. 3, pp. 278–288, Dec. 1999.

[23] E. Warner, D. B. Plewes, R. S. Shumak, G. C. Catzavelos, L. S. D. Prospero, M. J. Yaffe, V. Goel, E. Ramsay, P. L. Chart, D. E. Cole, G. A. Taylor, M. Cutrara, T. H. Samuels, J. P. Murphy, J. M. Murphy, and S. A. Narod, "Comparison of breast magnetic resonance imaging, mammography and ultrasound for surveillance of women at high risk for hereditary breast cancer," *J. Clin. Oncol.*, vol. 19, no. 15, pp. 3524–31, 2001.

[24] M. M. Burlew, E. L. Madsen, J. A. Zagzebski, R. A. Banajavic, and S. W. Sum, "A new ultrasound tissue-equivalent material," *Radiology*, vol. 134, pp. 517–520.

[25] D. C. Montgomery and G. C. Runger, *Applied Statistics and Probability for Engineers*. Toronto, ON, Canada: Wiley, 1994, pp. 803–830.

[26] C. K. Kuhl, "MRI of breast tumors," *Eur. Radiology*, vol. 10, pp. 46–58, 2000.

[27] T. Sumanaweera, G. Glover, S. Song, J. Adler, and S. Napel, "Quantifying MRI geometric distortion in tissue," *MRM*, vol. 31, pp. 40–47, 1994.

[28] S. Langlois, M. Desvignes, J. M. Constans, and M. Revenu, "MRI geometric distortion: A simple approach to correcting the effects of nonlinear gradient fields," *JMRI*, vol. 9, pp. 821–831, 1999.

[29] G. F. Lockwood, F. S. Foster, and J. W. Hunt, "A ray tracing method for calculating the speed of sound in a nonparallel layered model using pulse echo ultrasound," *Ultrason. Imag.*, vol. 11, pp. 106–118, 1989.

[30] ATL Ultrasound, Bothwell, WA, *HDI 5000 Ultrasound System Reference Manual* (4703-0027-03 Rev A), 2000, ch. 6-29.

[31] S. F. Foster and F. T. D'Astous, "Frequency dependence of ultrasound attenuation and backscatter in breast tissue," *Ultrasound Med. Biol.*, vol. 12, no. 10, pp. 795–808, 1986.

[32] R. R. Entrekin, B. A. Porter, H. H. Sillesen, and A. D. Wong, "Real-time spatial compounding imaging: Application to breast, vascular and musculoskeletal ultrasound," *Seminars Ultrasound CT MR*, vol. 22, pp. 50–64, 2001.

[33] T. J. Passe, D. A. Bluemke, and S. S. Siegelman, "Tumor angiogenesis: Tutorial on implications for imaging," *Radiology*, vol. 203, pp. 593–600, 1997.

[34] L. D. Buadu, J. Murakami, S. Murayama, N. Hashiguchi, S. Sakai, K. Masuda, S. Toyoshima, S. Kuroki, and S. Ohno, "Breast lesions: Correlation of contrast medium enhancement patterns on MR images with histopathologic findings and tumor angiogenesis," *Radiology*, vol. 200, pp. 639–649, 1996.

[35] C. M. Rumack, S. R. Wilson, and J. W. Charboneau, *Diagnostic Ultrasound*, 2nd ed. MO, Mosbey: St. Louis, 1998, vol. 1, ch. Ch. 3.

[36] G. Rizzatto and R. Chersevani, "Breast ultrasound and new technologies," *Eur. J. Radiol.*, vol. 27, pp. 242–249, 1998.

[37] S. Huber, T. Helbich, J. Kettenbach, W. Dock, I. Zuna, and S. Delorme, "Effects of a microbubble contrast agent on breast tumors: Computer-assisted quantitative assessment with color doppler US-early experience," *Radiology*, vol. 208, pp. 485–489, 1998.

[38] W. K. Moon, J. G. Im, D. Noh, and M. C. Han, "Nonpalpable breast lesions: Evaluation with power doppler US and a microbubble contrast agent—Initial experience," *Radiology*, vol. 217, pp. 240–246, 2000.